

Crossover from Elastic to Plastic Vortex Creep across the Second Magnetization Peak of High-Temperature Superconductors

著者	小池 洋二
journal or publication title	Physical review. B
volume	62
number	22
page range	15172-15176
year	2000
URL	http://hdl.handle.net/10097/35333

doi: 10.1103/PhysRevB.62.15172

Crossover from elastic to plastic vortex creep across the second magnetization peak of high-temperature superconductors

L. Miu

National Institute of Materials Physics, Bucharest-Magurele, MG-7, Romania

T. Noji and Y. Koike

Department of Applied Physics, Tohoku University, Aramaki Aoba, Aoba-ku, Sendai 980-77, Japan

E. Cimpoiasu, T. Stein, and C. C. Almasan

Department of Physics, Kent State University, Kent, Ohio 44242

(Received 5 April 2000; revised manuscript received 21 June 2000)

We investigated the relaxation of the irreversible magnetization of $\text{YBa}_2\text{Cu}_3\text{O}_{7-\delta}$, $\text{Pb}_2\text{Sr}_2\text{Y}_{0.53}\text{Ca}_{0.47}\text{Cu}_3\text{O}_8$, and $\text{Bi}_2\text{Sr}_2\text{CaCu}_2\text{O}_{8+\delta}$ single crystals with significant quenched disorder in the region of the second magnetization peak. It was found that for an applied magnetic field between the onset field and the peak field the relevant current-density dependence of the activation energy exhibits a sudden change, which can be interpreted as a crossover from elastic to plastic vortex creep. The evolution of this change with magnetic field illustrates the increase of the collective pinning barrier between the onset field and the peak field. The observed increase of the collective pinning barrier is limited by the plastic barrier at the peak field. This appears to be a general behavior, and may have important consequences on the interpretation of the thermally induced vortex phase transition at high magnetic fields.

I. INTRODUCTION

In the presence of an external magnetic field H , the vortex lines penetrating a superconducting sample from the surface into the bulk can be trapped on pinning centers, leading to a spatially inhomogeneous flux distribution and to a finite irreversible magnetization.¹ By increasing H , the interaction between vortices becomes stronger, and will counteract the pinning force. Thus, after the sample is fully penetrated by vortices, one expects the magnetization (in absolute value) to decrease with increasing H . However, it has been often observed that the magnetization of high-temperature superconductors (HTSC's) increases again upon further increase of H in a certain range.^{2,3} This behavior, known as the second magnetization peak (SMP), represents one of the most important controversial problems in vortex dynamics.

Many scenarios have been proposed for the occurrence of the SMP in HTSC's, involving, for example, surface barriers,² sample inhomogeneities,³ a crossover from bulk pinning to surface barriers,⁴ dynamic effects,⁵ a dimensional transition,⁶ a weak first-order vortex-lattice melting,⁷ layer decoupling,⁸ or vortex stacking.⁹ By considering the competition between the elastic energy of the vortex system and the pinning energy,^{10,11} it has been suggested that the SMP can result from a transition of a low-field quasiordered vortex phase to a disordered vortex solid at higher fields, induced by the quenched disorder.¹⁰⁻¹⁵ It is now believed that the effective pinning enhancement appears when the pinning energy generated by the quenched disorder overcomes the elastic energy of the vortex system.

Evidence for the existence of two distinct vortex-solid phases was previously obtained in neutron diffraction and μRS experiments,^{16,17} but the dynamic behavior of the disordered vortex solid above the SMP is still unclear. The in-

crease of the effective pinning when the pinning energy overcomes the elastic energy of the vortex system^{10,11} should lead to the conclusion that the high-field vortex phase is an elastic vortex glass.^{18,19} In this case, the pinning barrier should exhibit a specific increase when the current density J decreases.¹ Alternatively, the vortex phase above the SMP could behave as a plastic vortex solid, where the dissipation process is dominated by the plastic deformation of the vortex system, associated with the motion of dislocations in the vortex solid²⁰ and/or vortex cutting and reconnection in an entangled vortex phase.¹³

In this work, we investigated the J dependence of the pinning barriers involved in the dissipation process across the second magnetization peak of $\text{YBa}_2\text{Cu}_3\text{O}_{7-\delta}$, $\text{Pb}_2\text{Sr}_2\text{Y}_{0.53}\text{Ca}_{0.47}\text{Cu}_3\text{O}_8$, and $\text{Bi}_2\text{Sr}_2\text{CaCu}_2\text{O}_{8+\delta}$ single crystals, identified with the intrinsic variation of the activation energy in the magnetization relaxation with J . We found that the relevant J dependence of the activation energy exhibits a sudden change for H between the onset field and the peak field, which can be interpreted as a crossover from elastic to plastic vortex creep, first proposed in Ref. 20.

II. EXPERIMENTAL

The investigated specimens are a $3 \times 3 \times 1.5 \text{ mm}^3$ single-grain $\text{YBa}_2\text{Cu}_3\text{O}_{7-\delta}$ sample (YBCO),²¹ having the critical temperature $T_c = 90.9 \text{ K}$, a $0.7 \times 0.5 \times 0.1 \text{ mm}^3$ $\text{Pb}_2\text{Sr}_2\text{Y}_{0.53}\text{Ca}_{0.47}\text{Cu}_3\text{O}_8$ single crystal (PSYCCO) grown by the PbO-NaCl flux method,²² with $T_c = 76 \text{ K}$, and a $0.5 \times 0.5 \times 0.025 \text{ mm}^3$ $\text{Bi}_2\text{Sr}_2\text{CaCu}_2\text{O}_{8+\delta}$ (BSCCO) single crystal²³ grown by the self-flux method, with $T_c \approx 87 \text{ K}$. YBCO and PSYCCO have a relatively low anisotropy (the anisotropy parameter $\varepsilon \approx \frac{1}{10} - \frac{1}{5}$) and the normal-state resistivity of the order of $10^{-3} \Omega \text{ cm}$. These samples are attrac-

tive due to the fact that the SMP is observed up to close to T_c (where the fundamental superconducting lengths have a strong temperature variation), and the influence of the dimensional crossover in the vortex system on the SMP can be ruled out. (The peak field is roughly one order of magnitude lower than the crossover field $B_{cr} = \Phi_0 \varepsilon^2 / s^2$,¹ where s is the distance between the superconducting layers. This is not the case of BSCCO single crystals, for which the peak field approaches B_{cr} .⁶) Both the high disorder degree and the reduced anisotropy of YBCO and PSYCCO exclude a dominant role of geometrical and surface barriers. The effect of such barriers is also expected to be diminished in the BSCCO crystals grown by the self-flux method, which contain many growth defects. The T_c value and the location of the SMP indicate that the investigated BSCCO crystal is slightly overdoped.^{23,24}

The magnetization M (considered as the magnetic moment divided by the sample volume) was measured in zero-field-cooling conditions as a function of H , temperature T , and time t , using a Quantum Design SQUID magnetometer in the RSO mode, with the frequency of 1 Hz and the amplitude of 0.3 cm. The external magnetic field was oriented along the crystallographic c axis.

III. RESULTS AND DISCUSSION

The determination of T_c , exemplified for YBCO, is illustrated in Fig. 1(a). This was taken at the abrupt onset of the diamagnetic signal measured in zero-field-cooling conditions in a small H value. For the same sample, the H dependence of the irreversible magnetization M_{irr} and the location of the onset field H_{on} and the peak field H_p are shown in Fig. 1(b). In all cases, $M_{irr}(H)$ was extracted from the magnetic hysteresis curves $M(H)$ as $M_{irr}(H) = [M_+(H) - M_-(H)]/2$, where $M_+(H)$ and $M_-(H)$ represent the total magnetization measured in increasing and decreasing H , respectively. YBCO exhibits a broad SMP, similar to PSYCCO.²² This is not only the result of sample inhomogeneities and a nonuniform field distribution inside the crystal, since local magnetic measurements on relatively clean YBCO single crystals revealed the same behavior.^{15,20} In contrast, the onset of the SMP observed in local magnetic field measurements performed on relatively clean BSCCO single crystals was found to be very sharp.¹²

The temperature dependence of the peak field for YBCO and PSYCCO is shown in Fig. 2. Due to relatively large M values even at high T , it is better to consider the magnetic induction $B_p(H_p) \approx H_p + 4\pi M(H_p)(1 - D)$. The demagnetization factor ($D \approx 0.64$ for YBCO and ≈ 0.75 for PSYCCO) was extracted from the initial slope of the $M(H)$ curves. As can be seen, $B_p(T) \propto [1 - (T/T_c)^2]^{4/3}$, and this aspect will be discussed later. By difference, the peak field of our BSCCO crystal (detected up to 35 K) exhibits only a weak decrease with increasing temperature,²³ whereas for clean BSCCO single crystals B_p is temperature independent.^{12,15}

Figure 3(a) illustrates the relaxation curves, M_{irr} as a function of $\ln(t)$, for YBCO at $T = 75$ K and several H values in the SMP domain. As a rule, the first data point on the $M(t)$ curve, $M_+(H)$, and $M_-(H)$ were taken $t_1 = 100$ sec

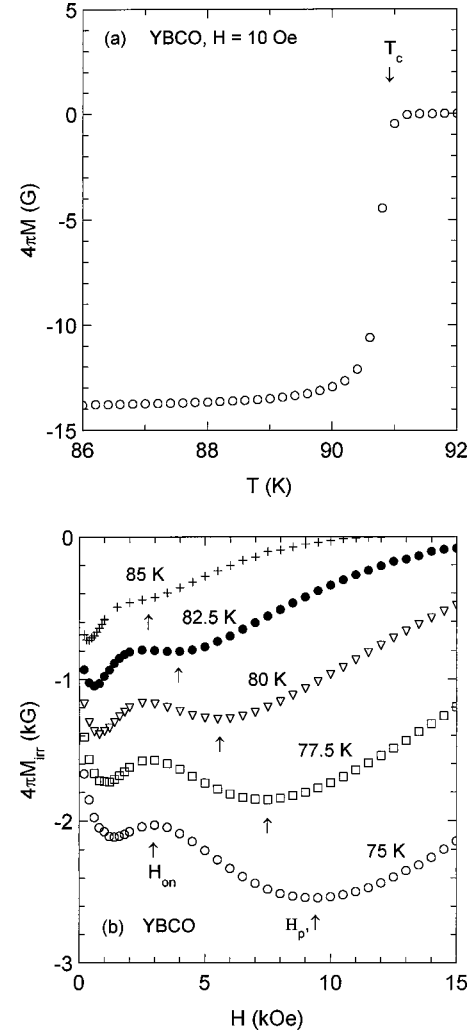


FIG. 1. (a) Magnetic transition of the $\text{YBa}_2\text{Cu}_3\text{O}_{7-\delta}$ crystal (YBCO) in a magnetic field $H = 10$ Oe applied along the crystallographic c axis in zero-field-cooling conditions. The critical temperature $T_c = 90.9$ K was taken at the abrupt onset of the diamagnetic signal. (b) Magnetic field dependence of the irreversible magnetization $M_{irr}(H)$ of the sample YBCO at several temperatures, revealing a broad second magnetization peak. The location of the onset field H_{on} and the peak field H_p is indicated by an arrow.

after the field was applied, to avoid the influence of flux redistribution in the initial stage of the relaxation process.²⁵ To obtain $M_{irr}(t)$, the measured $M(t)$ curve was shifted by $M(t_1) - M_{irr}(t_1)$, which contains the (nonrelaxing) reversible magnetization of the sample and the magnetization of the sample holder (also reversible).

It is tempting to determine the activation energy directly from the slope of the relaxation curve [Fig. 3(a)], which immediately leads to the intriguing conclusion that for H close to H_{on} the activation energy is larger than for H close to H_p (where $|M_{irr}|$ has its maximum [Fig. 1(b)]). As shown below, this is a direct consequence of the presence of elastic (collective) pinning barriers for $H \leq H_p$, with a strong J dependence.

As discussed in Ref. 25, the nonlinearity of the relaxation curves is one of the key points in the analysis of the magnetic relaxation data, reflecting the nonlinearity in the varia-

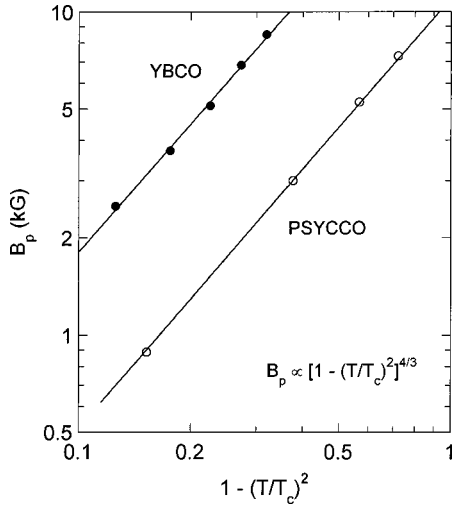


FIG. 2. The peak induction B_p of YBCO and the $\text{Pb}_2\text{Sr}_2\text{Y}_{0.53}\text{Ca}_{0.47}\text{Cu}_3\text{O}_8$ single crystal (PSYCCO) vs $1 - (T/T_c)^2$, in a double logarithmic plot. For both samples, $B_p(T) \propto [1 - (T/T_c)^2]^{4/3}$.

tion of the activation energy with J . The analysis of global magnetic relaxation data is rather difficult, since, in addition to the “intrinsic” (model-dependent) J dependence of the activation energy, there exists an “extrinsic” nonlinearity, mainly caused by the barrier distribution²⁶ and/or the spatial distribution of the critical-current density J_c .²⁷ It is well-known from the study of classical superconductors²⁸ that this distribution leads to power-law shaped voltage-current characteristics, which means that the activation energy is close to $U_0 \ln(J_c/J)$, where U_0 is constant.²⁹ Consequently, our approach is to consider that the effective activation energy $U(J)$ is of the form $U(J) = U_{\text{int}}(J) \ln(J_c/J)$, where $U_{\text{int}}(J)$ represents the relevant intrinsic J dependence of the activation energy.

The behavior of $U_{\text{int}}(J)$ can be found by analyzing the J dependence of an “activation energy” U^* determined from the relaxation curves as

$$U^* = -T[d \ln |M_{\text{irr}}| / d \ln(t)]^{-1}. \quad (1)$$

With the general equation $U(J) = T \ln(t/t_0)$ (Ref. 25) (where t_0 is a macroscopic quantity of the order of milliseconds, referred to as the “effective” hopping attempt time) and $J \propto |M_{\text{irr}}|$, one can easily derive the relation between $U^*(J)$ and $U_{\text{int}}(J)$. When U_{int} has a weak J dependence, as in the case of the plastic barriers U_{pl} , $U^*(J) = U_{\text{int}}(J) - J \ln(J_c/J) dU_{\text{int}}/dJ \approx U_{\text{int}}(J)$. For elastic vortex creep, $U_{\text{int}}(J)$ at low J should be given by the elastic barrier $U_{\text{el}}(J) \approx U_c (J_c/J)^\mu$,³⁰ where U_c is the collective pinning barrier and the collective pinning exponent $\mu \approx 1$. In this situation, one obtains $U^*(J) = U_{\text{el}}(J) [\mu \ln(J_c/J) + 1]$.

Figure 3(b) shows the resulting $U^*(J)$ dependence across the SMP of YBCO at $T=75$ K. For H between $H_{\text{on}} (\approx 3 \text{ kOe})$ and $H_p (\approx 9.4 \text{ kOe})$, there is a first rapid increase of U^* with decreasing J , resembling elastic vortex creep. At lower J , this is replaced by a slower $U^*(J)$

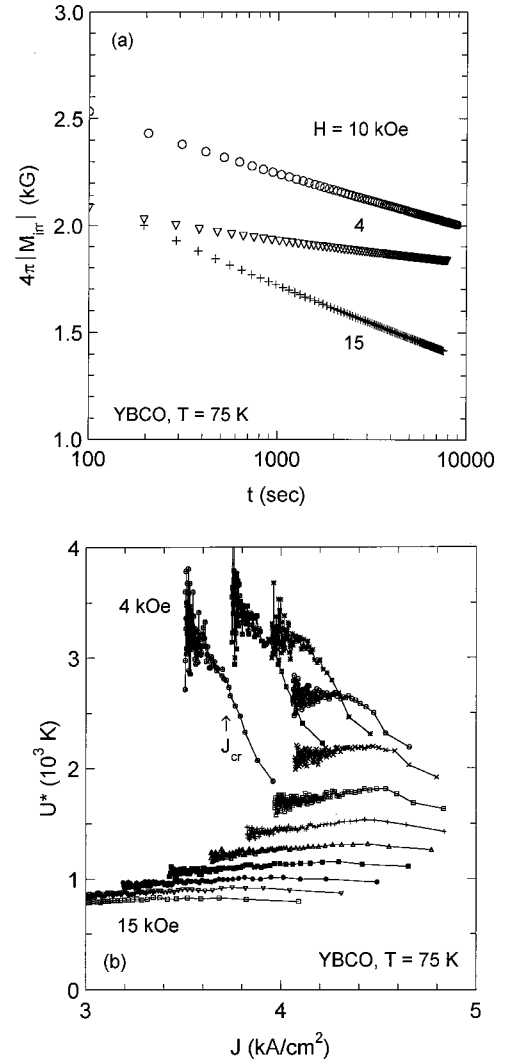


FIG. 3. (a) Relaxation of the irreversible magnetization M_{irr} of YBCO at $T=75$ K for an applied magnetic field H just above the onset field ($H=4$ kOe), close to the peak field ($H=10$ kOe), and above the peak field [$H=15$ kOe, see Fig. 1(b)]. (b) Current-density J dependence of the activation energy U^* determined with Eq. (1) across the second magnetization peak of YBCO at $T=75$ K (H was increased by 1 kOe). Up to the peak field (≈ 10 kOe), there is a first rapid increase of U^* with decreasing J , signaling elastic vortex creep. At a certain J value (J_{cr}), indicated by an arrow for the first H value, there is a crossover toward a weaker $U^*(J)$ variation, attributed to plastic vortex creep. Above the peak field, only a weak $U^*(J)$ variation was observed.

variation, characteristic for plastic vortex creep. This change appears at a certain current density J_{cr} , when $U_{\text{el}}(J_{\text{cr}}) = U_{\text{pl}}(J_{\text{cr}})$.

For $H > H_p$, only a weak $U^*(J)$ dependence is observed [Fig. 3(b)], suggesting that the creep process is predominantly plastic. The slight decrease of U^* with decreasing J in the plastic creep region seems to result mainly from the above difference between $U^*(J)$ and $U_{\text{int}}(J)$ (with $dU_{\text{int}}/dJ < 0$), rather than from the increase of B inside the sample during the magnetization relaxation.

The change of the $U^*(J)$ variation for H below and above H_p appears to be a general behavior. This is illustrated for

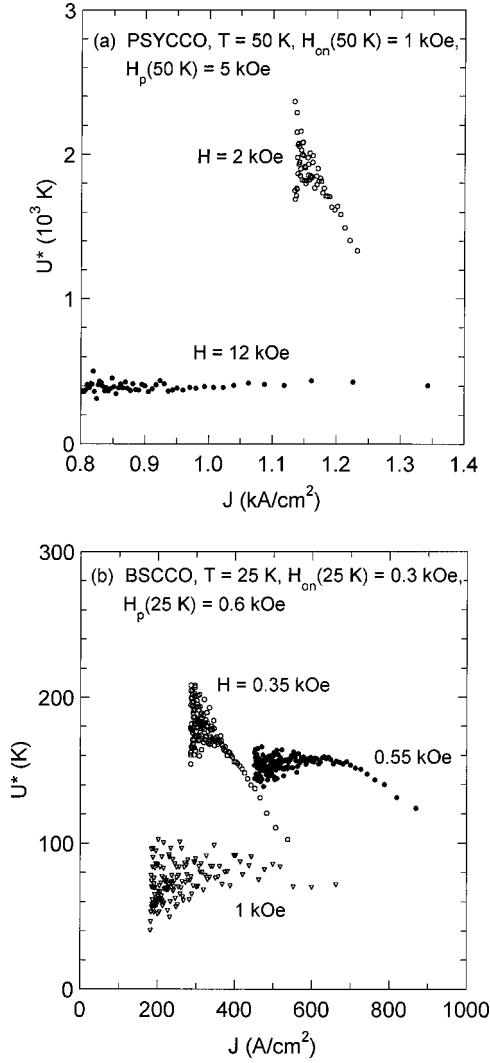


FIG. 4. Characteristic $U^*(J)$ variation for the applied magnetic field H between the onset field H_{on} and the peak field H_p , and above H_p , illustrated for PSYCCO at $T=50$ K (a), and the $\text{Bi}_2\text{Sr}_2\text{CaCu}_2\text{O}_{8+\delta}$ single crystal (BSCCO) grown by the self-flux technique at $T=25$ K (b).

PSYCCO at $T=50$ K in Fig. 4(a), and for BSCCO at $T=25$ K in Fig. 4(b). It is worth noting that in the case of clean BSCCO single crystals the change in the relaxation process at the SMP was attributed in Ref. 4 to a crossover from a bulk pinning to a surface-barrier regime of dissipation. However, the behavior of our BSCCO single crystal grown by the self-flux technique [Fig. 4(b)] is similar to that exhibited by YBCO [Fig. 3(b)], where the role of the surface barriers should be small.

The evolution of the initial upward curvature of $U^*(J)$ with increasing H between H_{on} and H_p [Figs. 3(b) and 4(b)] indicates an increase of U_c , in agreement with recent models involving the enhancement of the effective pinning when the pinning energy generated by the quenched disorder overcomes the elastic energy of the vortex system.^{10,11} Actually, the U_c enhancement should be more pronounced, since the determined $U^*(J)$ overestimates $U_{el}(J)$ by the factor $[\mu \ln(J_c/J)+1]$, which is larger for H close to H_{on} . The rapid $U^*(J)$ variation for H just above H_{on} , in qualitative agree-

ment with $U_{el}(J)$, can explain the peculiar behavior of the slope of the relaxation curves from Fig. 3(a), as well as the attenuation of the SMP when the waiting time t_1 is shortened, or at low T . When T is not too low, the high- J states (for which U_{el} is small) will relax in the time interval from $t=0$ to t_1 . The different relaxation rates below and above H_p make the peak field time dependent [Fig. 3(b)].

If one takes $\Delta \ln U^*/\Delta \ln(J)$ in the J domain where $U^*(J)$ exhibits the upward curvature, the resulting exponent decreases continuously with H , and becomes ≈ 0.5 in the vicinity of H_p . This practically reproduces the value obtained in Ref. 20, using local magnetic field measurements, since the influence of the factor $[\mu \ln(J_c/J)+1]$ on this exponent is weak close to H_p . A low exponent μ around H_p means a single-vortex collective pinning regime, which points toward a continuous destruction of the quasi-ordered vortex phase across the SMP.

Finally, we discuss the $B_p(T)$ variation illustrated in Fig. 2. For the investigated samples (with a relatively high disorder degree), the energy of thermal fluctuations can be neglected in the considered T interval. This is supported by the fact that there is no upturn in $B_p(T)$ at high T . With the above considerations, the $B_p(T)$ dependence should result from the equality between the single vortex depinning energy, $\propto (\gamma \varepsilon \varepsilon_0 \xi^4)^{1/3}$, and the plastic barrier $U_{pl} \approx \varepsilon \varepsilon_0 a_0$.¹ The energy scale $\varepsilon_0 = (\Phi_0/4\pi\lambda)^2$, where λ is the magnetic penetration depth, ξ is the coherence length, γ is the disorder parameter, and a_0 is the mean intervortex spacing. $\xi(T)$ and $\varepsilon_0(T)$ are general, but $\gamma(T)$ is pinning dependent. For a δT_c pinning, which originates from local suppressions of T_c , $\gamma \propto \lambda^{-4}$,¹ leading to

$$B_p(T) \propto [1 - (T/T_c)^2]^{4/3}, \quad (2)$$

as observed.

IV. CONCLUSIONS

In summary, the analysis of the relevant current-density dependence of the activation energy in the magnetization relaxation of YBCO, PSYCCO, and BSCCO single crystals with significant quenched disorder reveals a crossover from elastic to plastic vortex creep for H between H_{on} and H_p , which appears to be a general behavior. The existing differences between the SMP exhibited by highly anisotropic HTSC's, such as BSCCO, and by less anisotropic HTSC's, such as YBCO, are due to the fact that in the case of relatively clean BSCCO single crystals the peak field is limited by the crossover field B_{cr} , which can explain the weak $B_p(T)$ dependence. Around B_{cr} , the elastic moduli of the vortex system suddenly decrease,¹ generating a very sharp onset of the SMP in local magnetic field measurements.¹²

The observed increase of the collective pinning barrier across the SMP is limited by the plastic barrier at B_p , and the creep process above B_p becomes predominantly plastic. The large amount of plastic vortex creep in HTSC's at high magnetic fields may have important consequences on the interpretation of the thermally induced vortex solid-vortex

fluid transition. The existence of a viscous vortex liquid was signaled in HTSC's with relatively low anisotropy,³¹ as well as in BSCCO with significant quenched disorder,³² in agreement with the theoretical prediction.³³ These results suggest that the thermally induced vortex-phase transition in the high-field region should be consistent with a continuous "freezing" of a viscous vortex fluid into a plastic vortex solid.

ACKNOWLEDGMENTS

This work was supported by the National Science Foundation under Grant No. DMR-9801990 at Kent State University, and by the Japan Society for Promotion of Science at Tohoku University. The kind assistance of the Alexander von Humboldt Foundation is gratefully acknowledged.

- ¹G. Blatter, M. V. Feigel'man, V. B. Geshkenbein, and V. M. Vinokur, *Rev. Mod. Phys.* **66**, 1125 (1994), and references therein.
- ²V. N. Kopylov, A. E. Koshelev, I. F. Schegolev, and T. G. Tognidze, *Physica C* **223**, 291 (1990).
- ³M. Daeumling, J. M. Seuntjens, and D. C. Larbalestier, *Nature (London)* **346**, 332 (1990).
- ⁴N. Chikumoto, M. Konczykowski, N. Motohira, and A. P. Malozemoff, *Phys. Rev. Lett.* **69**, 1260 (1992).
- ⁵L. Krusin-Elbaum, L. Civale, V. M. Vinokur, and F. Holtzberg, *Phys. Rev. Lett.* **69**, 2280 (1992).
- ⁶T. Tamegai, I. Oguro, Y. Iye, and K. Kishio, *Physica C* **223**, 33 (1993).
- ⁷J. Shi, X. S. Ling, R. Liang, D. A. Bonn, and W. N. Hardy, *Phys. Rev. B* **60**, R12 593 (1999).
- ⁸B. Horovitz, *Phys. Rev. B* **60**, R9939 (1999).
- ⁹D. K. Jackson, M. Nicodemi, G. Perkins, N. A. Lindop, and H. J. Jensen, cond-mat/9908454 (unpublished).
- ¹⁰T. Giamarchi and P. Le Doussal, *Phys. Rev. Lett.* **72**, 1530 (1994); *Phys. Rev. B* **55**, 6577 (1997); V. Vinokur, B. Khaykovich, E. Zeldov, M. Konczykowski, R. A. Doyle, and P. Kes, *Physica C* **295**, 209 (1998); J. Kierfeld, *ibid.* **300**, 171 (1998).
- ¹¹D. Ertas and D. R. Nelson, *Physica C* **272**, 79 (1996).
- ¹²B. Khaykovich, E. Zeldov, D. Majer, T. W. Li, P. H. Kes, and M. Konczykowski, *Phys. Rev. Lett.* **76**, 2555 (1996).
- ¹³D. Giller, A. Shaulov, R. Prozorov, Y. Abulafia, Y. Wolfus, L. Burlachkov, Y. Yeshurun, E. Zeldov, V. M. Vinokur, J. L. Peng, and R. L. Green, *Phys. Rev. Lett.* **79**, 2542 (1997).
- ¹⁴K. Deligiannis, P. A. J. de Groot, M. Oussena, S. Pinfold, R. Langan, R. Gagnon, and L. Taillefer, *Phys. Rev. Lett.* **79**, 2121 (1997).
- ¹⁵D. Giller, A. Shaulov, Y. Yeshurun, and J. Giapintzakis, *Phys. Rev. B* **60**, 106 (1999).
- ¹⁶R. Cubitt, E. M. Forgan, G. Yang, S. L. Lee, D. M. Paul, H. A. Mook, M. Yethiraj, P. H. Kes, T. W. Li, A. A. Menovsky, Z. Tarnawski, and K. Mortensen, *Nature (London)* **365**, 407 (1993).
- ¹⁷S. L. Lee, P. Zimmermann, H. Keller, M. Warden, I. M. Savic, R. Schauwecker, D. Zech, R. Cubitt, E. M. Forgan, P. H. Kes, T. W. Li, A. A. Menovsky, and Z. Tarnawski, *Phys. Rev. Lett.* **71**, 3862 (1993).
- ¹⁸R. H. Koch, V. Foglietti, W. J. Gallagher, G. Koren, A. Gupta, and M. P. A. Fisher, *Phys. Rev. Lett.* **63**, 1511 (1989); P. L. Gammel, L. F. Schneemeyer, and D. J. Bishop, *ibid.* **66**, 953 (1991).
- ¹⁹G. Blatter, *Physica C* **282–287**, 19 (1997); T. Nishizaki, T. Naito, and N. Kobayashi, *Phys. Rev. B* **58**, 11 169 (1998).
- ²⁰Y. Abulafia, A. Shaulov, Y. Wolfus, R. Prozorov, L. Burlachkov, Y. Yeshurun, D. Majer, E. Zeldov, H. Wühl, V. B. Geshkenbein, and V. M. Vinokur, *Phys. Rev. Lett.* **77**, 1596 (1996).
- ²¹The Y-123 crystal was grown by C. Beduz at the Institute of Cryogenics, Southampton.
- ²²T. Noji, Y. Koike, K. Ohtsubo, S. Shiga, M. Kato, A. Fujiwara, and Y. Saito, *Jpn. J. Appl. Phys.* **33**, 2515 (1994); T. Noji, T. Takabayashi, M. Kato, T. Nishizaki, N. Kobayashi, and Y. Koike, *Physica C* **255**, 10 (1995); T. Noji, T. Takabayashi, T. Nishizaki, N. Kobayashi, and Y. Koike, *ibid.* **263**, 442 (1996).
- ²³L. Miu, E. Cimpoiasu, T. Stein, and C. C. Almasan, *Physica C* **334**, 1 (2000).
- ²⁴S. Ooi, T. Shibauchi, and T. Tamegai, *Physica C* **302**, 339 (1998).
- ²⁵Y. Yeshurun, A. P. Malozemoff, and A. Shaulov, *Rev. Mod. Phys.* **68**, 911 (1996), and references therein.
- ²⁶R. Griessen, *Phys. Rev. Lett.* **64**, 1674 (1990).
- ²⁷J. Z. Sun, C. B. Eom, B. Lairson, J. C. Bravman, and T. H. Geballe, *Phys. Rev. B* **43**, 3002 (1991).
- ²⁸W. H. Warnes and D. C. Larbalestier, *Appl. Phys. Lett.* **48**, 1403 (1986).
- ²⁹E. Zeldov, N. M. Amer, G. Koren, A. Gupta, M. W. McElfresh, and R. J. Gambino, *Appl. Phys. Lett.* **56**, 680 (1990).
- ³⁰M. V. Feigel'man, V. B. Geshkenbein, A. I. Larkin, and V. M. Vinokur, *Phys. Rev. Lett.* **63**, 2303 (1989); D. S. Fisher, M. P. A. Fisher, and D. A. Huse, *Phys. Rev. B* **43**, 130 (1991).
- ³¹D. Lopez, L. Krusin-Elbaum, H. Safar, E. Righi, F. de la Cruz, S. Grigera, C. Field, W. K. Kwok, L. Paulinus, and G. W. Crabtree, *Phys. Rev. Lett.* **80**, 1070 (1998).
- ³²L. Miu, G. Jakob, P. Haibach, F. Hillmer, C. C. Almasan, and H. Adrian, *Phys. Rev. B* **57**, 3151 (1998).
- ³³V. M. Vinokur, M. V. Feigel'man, V. B. Geshkenbein, and A. I. Larkin, *Phys. Rev. Lett.* **65**, 259 (1990).